sProceedings of the 28th International Conference on Ocean, Offshore and Arctic Engineering
OMAE 2009
May 31-June 5, 2009, Honolulu, Hawaii, USA

OMAE2009-79598

BEYOND WAVES AND SPECTRA: EULER CHARACTERISTICS OF OCEANIC SEA STATES

Francesco Fedele
School of Civil & Environmental Engineering
Georgia Institute of Technology, USA

G. Gallego, A. Yezzi
School of Electrical & Computer Engineering,
Georgia Institute of Technology, USA

A. Benetazzo
Protecno S.r.l. Padua ITALY

M. A. Tayfun
College of Engineering, Kuwait University, Kuwait

G. Z. Forristall
Forristall Ocean Engineering, Inc. USA

L. Cavaleri, M. Sclavo, M. Bastianini
ISMAR-CNR, Venice, Italy

ABSTRACT

We present an application of a novel variational Wave Acquisition Stereo System (**WASS**) for the estimation of the space-time dynamics of oceanic sea states. **WASS** technology, if combined with statistical techniques of the Euler Characteristics of random excursion sets, provides a new paradigm for the accurate prediction of the largest crest expected over an area.

INTRODUCTION

The prediction of large waves is typically based on the statistical analysis of time series of the wave surface displacement retrieved from wave gauges, ultrasonic instruments or buoys at a fixed point P of the ocean. However, the largest wave crest predicted in time at P underestimates the highest crest expected over the area nearby P. Indeed, large waves travel on top of wave groups, and the probability that the group passes at its apex through P is practically null. The large crest height recorded in time at P is simply due to the dynamical effects of a group that focuses nearby that location forming a larger wave crest. Can we predict the largest wave expected over a given area? Yes we can if the exceedance probability

$$\Pr\left(\max_{P\in S}\eta(P) > h\right) \qquad (1)$$

of the global maximum of the wave surface η over a given area S is known. Asymptotic solutions of (1) for Gaussian fields are given by Piterbarg (1995) in the limit of an infinite area, and by Adler (1981) and Adler & Taylor (2007) exploiting Euler Characteristics (EC) of random excursion sets. These theoretical results are very useful for ocean & coastal engineering design. Indeed, Socquet-Juglard et al. (2005) applied Piterbarg's theorem to explain large spatial waves observed in simulations of the Dysthe equation. Further, Forristall (2006) used Piterbarg's results to explain the damages sometimes observed on the lower decks of platforms after storms (Forristall 2007). These may be due to a design that underestimates the largest crest height expected over the area nearby the offshore structure. Offshore industry can thus benefit from the synergy of technologies and statistical tools that provide *predictions of the largest wave expected over a given area and the associated spectral properties.*

In this paper, we present a ***W**ave **A**cquisition **S**tereo **S**ystem* (**WASS**), a video observational technology able to acquire four-dimensional (4D) video data (both in space and time) of oceanic states. The rich statistical content of 4D data allows reliable estimates of the expected global maximum (largest crest height) over an area via Euler Characteristics' theory (Adler 1981, Adler & Taylor 2007).

WASS has a significant advantage as a low-cost system in both installation and maintenance. Further, it provides spatial and temporal data whose statistical content is richer than that of a time series retrieved from a buoy, which is expensive to install and maintain. **WASS** exploits the combination of state-of-the-art of epipolar methods (Benetazzo 2006) and variational partial differential equation techniques (Jin et al. 2005) for the 4D stereo reconstruction of the spatio-temporal dynamics of ocean waves. We have preliminary results

(Gallego et al. 2008) showing that **WASS** yields accurate estimates of the spatio-temporal ocean dynamics, the associated wave spectra and wave surface statistics.

The paper is structured as follows. We first briefly review the theory behind the variational **WASS** and then introduce the EC of excursion sets of random fields. We then analyze the *EC* of spatial snapshots η of oceanic sea states acquired via **WASS**. We present new estimates from video data of both directional wave spectra and empirical exceedance probabilities of the global maximum of η over an area. The broader impact of these results to oceanic applications is also discussed.

THE STEREO VARIATIONAL GEOMETRIC METHOD

The reconstruction of the wave surface from stereo pairs of ocean wave images is a classical problem in computer vision commonly known as the correspondence problem (Ma et al. 2004). For **WASS** we solve this by two distinct approaches based on epipolar geometries and variational techniques. In the former, the 'epipolar algorithm' of Benetazzo (2006) finds corresponding points in the two images, from which the estimate of the real point in the three dimensional terrestrial coordinate system can be obtained. However, this approach may fail to provide a smooth surface reconstruction because of "holes" corresponding to unmatched image regions (Ma et al. 2004, Benetazzo 2006). This is typical during cloudy days, when at a given point on the water surface, the same amount of light is received from all possible directions and reflected towards the observer causing a visual blurring of the specularities of the water. In this case, the water surface is said to support a Lambertian radiance function (Ma et al. 2004). Variational techniques overcome this problem. Under the assumptions of a Lambertian surface, following the seminal work by (Faugeras et al. 1998), the 3-D reconstruction of the water surface is obtained in the context of active surfaces by evolving an initial surface through a PDE derived from the gradient descent flow of a cost functional designed for the stereo reconstruction problem.

To be more specific, the energy being *maximized* is the normalized cross correlation between the image intensities obtained by projecting the same water surface patch onto both image planes of the cameras. It is clear that such energy depends on the shape of the water surface. Therefore, the active surface establishes an evolving correspondence between the pixels in both images. Hence, the correspondence will be obtained by evolving a surface in 3-D instead of just performing image-to-image intensity comparisons without an explicit 3-D model of the target surface being reconstructed.

To infer the shape of the water surface $\eta(x,y)$ at the location *(x,y)* over an area *S*, we set up a cost functional on the discrepancy between the projection of the model surface and the image measurements. As previously announced, such cost is based on a cross correlation measure between image intensities, which will be noted as $E_{\text{data}}(\eta)$. We conjecture that, to have a well-posed problem, a regularization term that imposes a geometric prior must also be included, $E_{\text{geom}}(\eta)$. We consider the cost functional to be the (weighted) sum:

$$E(\eta) = E_{data}(\eta) + E_{geom}(\eta). \qquad (2)$$

In particular, the geometric term favors surfaces of least area:

$$E_{geom}(\eta) = \int_{\eta} dA\,. \qquad (3)$$

The data fidelity term may be expressed as

$$E_{data}(\eta) = \int_{\eta}\left(1 - \frac{\langle I_1, I_2\rangle}{|I_1|\cdot|I_2|}\right)dA\,, \qquad (4)$$

where η is the wave surface region within the field of views of both cameras, and $\langle I_1, I_2\rangle$ is the cross-correlation between the image intensities I_1 and I_2.

The surface η is found by minimizing *E* via a gradient flow-based iterative algorithm that starts from an initial estimate of the surface at time $t = 0$, η_0, and it will make the surface evolve towards a minimizer of *E*, hopefully converging to the desired water surface shape. Based on the theorem in (Faugeras et al. 1998) that says that for a function $\Phi : R^3 \times R^3 \rightarrow R^+$ and the energy

$$E = \int_{\eta} \Phi(X, N)\,dA\,, \qquad (5)$$

where *N* is the unit normal to η at *X*, the flow that minimizes *E* is given by the evolution PDE

$$\eta_t = \beta N\,, \qquad (6)$$

where η_t is the derivative of η with respect to a fictitious time variable and the speed β in the normal direction to the surface that drives the evolution is

$$\begin{aligned}\beta = {} & 2H(\Phi - \Phi_N \cdot N) - \Phi_X \cdot N - \\ & + trace\left[(\Phi_{XN})_{T_\eta} + dN \circ (\Phi_{NN})_{T_\eta}\right]\end{aligned} \qquad (7)$$

All quantities are evaluated at the point $\eta = X$ with normal *N* to the surface. *H* denotes the mean curvature. Φ_X, Φ_N are the first-order derivatives of Φ, while Φ_{XN}, Φ_{NN} are the second-order derivatives. dN is the differential of the Gauss map of the surface and $(\cdot)_{T_\eta}$ means "restriction to the tangent plane T_η to the surface at η=*X*". Note that our proposed energy (2) can be expressed in the form of (5) if $\Phi = \left(1 - \langle I_1, I_2\rangle / |I_1|\cdot|I_2|\right) + \alpha$, where α is just a weight for the geometric prior. In practice, we use the flow based on the first-order derivatives of Φ because it provides similar results to those of the complete expression, but saves a significant amount of computations,

$$\eta_t = \left(2H(\Phi - \Phi_N \cdot N) - \Phi_X \cdot N\right)N. \qquad (8)$$

The level set framework has been adopted to numerically implement (8) (see Gallego et al. 2008). We have tested the variational reconstruction algorithm using a set of images, shown in the upper panel of Fig. 1, acquired by Benetazzo (2006) on a water depth of 8 meters. In the lower panel of the same figure it is shown the successful reconstructed surface. The associated directional and omni-directional wave spectra are shown in figure 2. Note that the spectrum tail decays as $k^{-2.5}$ in agreement with wave turbulence theory (Zakharov 1999) and the numerical simulations of the Dysthe equations (Socquet-Juglard et al. 2005). Hereafter, we introduce the concept of the Euler characteristic (*EC*) that will be applied to predict the expected number of large maxima in we oceanic sea states exploiting the high statistical content of the acquired video data via **WASS**.

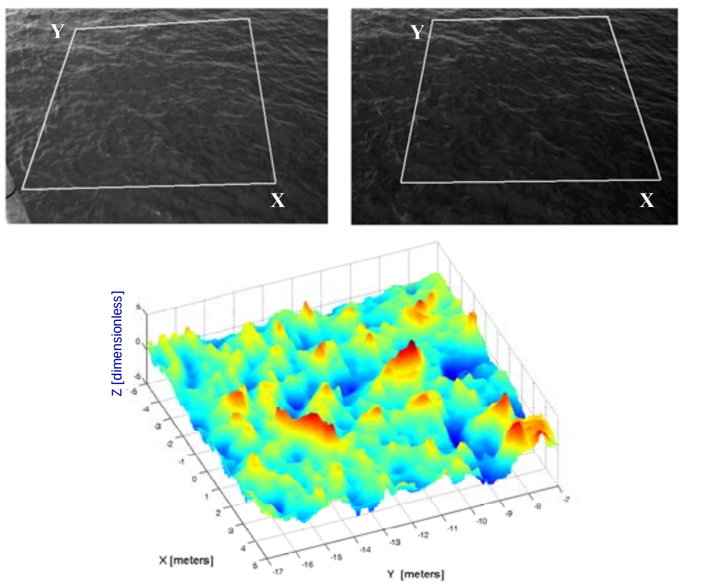

Figure 1: (Upper panel) Input stereo pair images to the algorithm. The rectangular domain (8 m x 8.7 m) of the reconstructed surface has been superimposed. The wave height is in the range ±0.2 m. (Lower panel) Reconstructed normalized wave surface η via **WASS**.

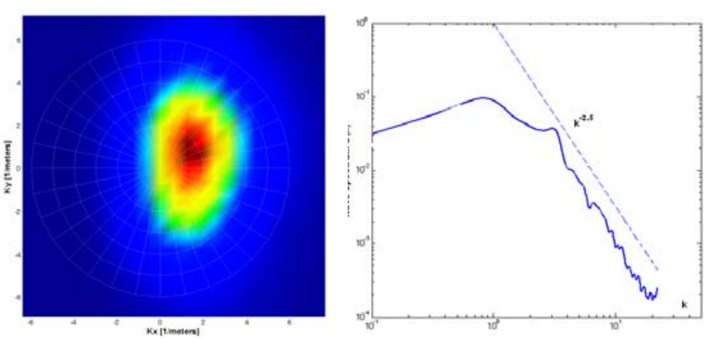

Figure 2: (left) Estimate of the directional wave spectrum of η of figure 1. (right) Omnidirectional spectrum with tail decaying as $k^{-2.5}$ (Socquet-Juglard et al. 2005, Zakharov 1999).

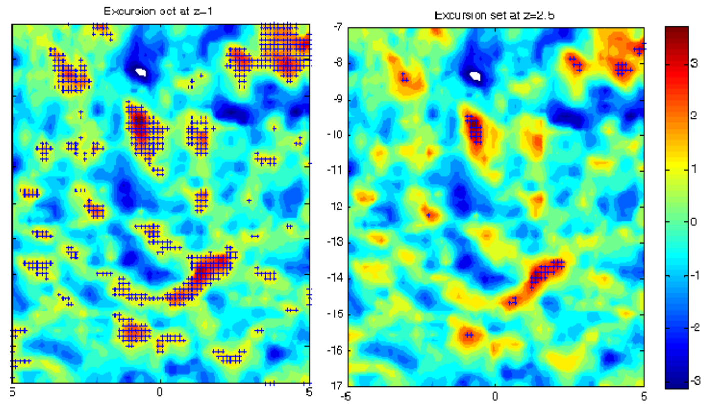

Figure 3: Excursion sets of a normalized zero-mean Gaussian field Z at the thresholds z=1 (left) and z=2.5 (right).

EULER CHARACTERISTICS

In algebraic topology, the **Euler characteristic** *EC* is classically defined for polyhedra according to the formula

$$EC = V - E + F\,, \tag{9}$$

where V, E, and F are respectively the numbers of vertices, edges and faces in the given polyhedron. The same definition given in (9) can be adapted to 2D surfaces which are the focus of this paper. In this case, the *EC* is also equivalent to the difference between the number connected components (CC) and holes (H) of the given set, viz.

$$EC = CC - H. \tag{10}$$

For a generic 2D set Σ with complicated regions, computing the *EC* from the definition (10) presents some challenges. A computationally efficient approach can be devised based on (9). Following Adler (1981), we first define a Cartesian mesh grid Γ of size (Δx, Δy) that approximates the complicated domain of the given set Σ. The *EC*(Γ) is then computed as follows. Denote F as the number of squares (faces) composing Γ, E_h (E_v) as the number of horizontal (vertical) segments between two neighboring mesh points and V the number of grid points. The *EC*(Γ) then follows from (9) setting $E = E_h + E_v$. As the grid cell size ΔxΔy tends to zero, *EC*(Γ) → *EC*(Σ). For example, for a square *EC*=4-4+1=1 according to (9), which is in agreement with (10) since there is only 1 connected component and no holes.

Consider now a two dimensional (2D) random field η to model realizations of oceanic sea states at fixed time (snapshots) over a given area S as in Figure. 3. The excursion set

$$A_{\eta,h} = \{(x, y) \in S : \eta(x, y) > h\}$$

is the portion of the area S above the threshold h. From Figure 3 it is clear that the *EC* of an excursion set depends very strongly on h. If this is low, then *EC* counts the number of holes in the given set. If the threshold is high (see Figure 3, right panel), then all the holes tend to disappear and the *EC* counts the number of connected components, or local maxima of the random field. For a stationary Gaussian field η, an exact formula for the expected value of *EC*, valid for any threshold, was discovered by Adler (1981). For 2D Gaussian fields defined over the region *S* of area A_S

$$\overline{EC(A_{\eta,h})} = A_S\, N_w \xi\, e^{-\xi^2/2}\,, \tag{11}$$

where $\overline{(\bullet)}$ means expectation , $\xi = h/\sigma$ is the normalized threshold amplitude, σ is the standard deviation of η and

$$N_w = (2\pi)^{-3/2}\sigma^{-2}|\mathbf{\Lambda}|^{1/2} \tag{12}$$

is the number of 'waves' per unit area with $\mathbf{\Lambda}$ as the covariance matrix of the gradient $\nabla\eta$. If the excursion set touches the boundary of the area *S*, correction terms need to be added (Worsley 1995). Why the *EC* of random excursion sets is relevant to oceanic applications?

Adler (1981) and Adler & Taylor (2007) have shown that the probability that the global maximum of a random field η exceeds a threshold *h* is well approximated by the expected *EC* of the excursion set $A_{\eta,h}$, provided the threshold is high. Indeed, as the threshold *h* increases, the holes in the excursion set $A_{\eta,h}$ disappear until each of its connected components includes just one local maximum, and the *EC* counts the number of local maxima. For very large thresholds, the *EC* equals 1 if the global maximum exceeds the threshold and 0 if it is below. Thus, the $EC(A_{\eta,h})$ of large excursion sets is a binary random variable with states 0 and 1, and for *h*>>1

$$\Pr\left(\max_{P\in S}\eta(P) > h\right) = \Pr\left[EC(A_{\eta,h}) = 1\right] = \overline{EC(A_{\eta,h})}\,. \tag{13}$$

Piterbarg (1995) also derived (13) by studying large Gaussian maxima over an infinite area, as $A_S \to \infty$. The global maximum of η is the largest wave crest expected over the area *S*. Thus, (13) provides the basis for accurate estimates of exceedance probabilities of large waves by means of the *EC* of excursion sets of video images retrieved via **WASS** (see Figure 1). A consequence of (13) is that, for *h*>>1

$$EX_{\max}(h) \approx \overline{EC(A_{\eta,h})}, \tag{14}$$

that is, the expected number $EX_{\max}$ of large local maxima greater than *h* equals the expected *EC* of large excursion sets.
This statement can be readily proved as follows (Aldous 1989). For a very large threshold *h*, the excursion set $A_{\eta,h}$ of a Gaussian field η(*x,y*) is the union of isolated connected components of all the local maxima above *h* (see Figure 4).

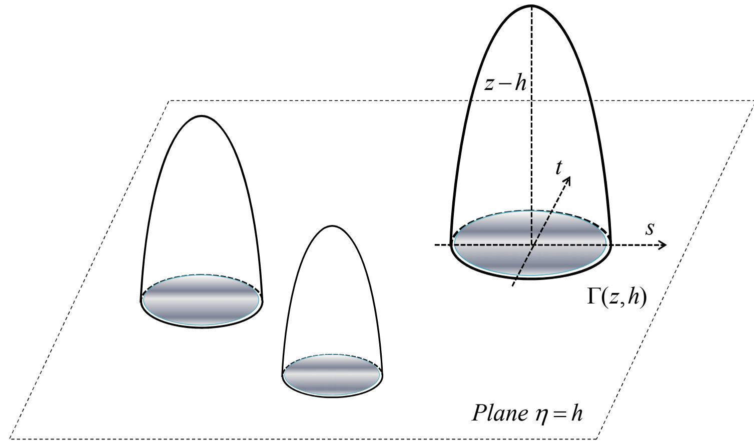

Figure 4: A typical excursion set $A_{\eta,h}$ of a gaussian field η(*x,y*), above a very large threshold *h*.

Define $EX_{lm}(z)dz$ as the number of local maxima with height in [*z,z+dz*] so that the expected number $EX_{\max}(h)$ of maxima larger than *h* follows as

$$EX_{\max}(h) = \int_h^\infty EX_{lm}(z)dz. \tag{15}$$

Further, call $\Gamma(z,h)$ the area covered by a local maximum of amplitude *z*>*h* intersecting with the plane *η*=*h* (see figure 5). The wave surface around this maximum that occurs at, say, $t = t_0$ and $s = s_0$, is described by the conditional Slepian model (Kac & Slepian 1959, Lindgren 1970,1972, Boccotti 2000)

$$\eta_c = \left\{\eta(t,s)\,\middle|\,\eta(t_0,s_0) = z\right\} = \frac{z}{\sigma^2}\Psi(t-t_0, s-s_0) + R\,, \tag{16}$$

where (*t,s*) are the principal directions of η, Ψ is the covariance and *R* is a random residual of O(z^0). For *z*>>1, *R* can be neglected and Taylor-expanding (20) nearby $t = t_0$, $s = s_0$ yields

$$\eta_c = z - z\left(\frac{m_{tt}}{2\sigma^2}(t-t_0)^2 + \frac{m_{ss}}{2\sigma^2}(s-s_0)^2 + \ldots\right). \tag{17}$$

Setting $\eta_c = h$, $\Gamma(z,h)$ follows from (21) as the area of the ellipse of equation

$$\frac{(t-t_0)^2}{A^2} + \frac{(s-s_0)^2}{B^2} = 1\,,$$

with semi-axises given by

$$A = \sigma\sqrt{2\frac{z-h}{h\,m_{tt}}}\,,\quad B = \sigma\sqrt{2\frac{z-h}{h\,m_{ss}}}\,.$$

Thus,

$$\Gamma(z,h) = \pi AB = \frac{2\pi\sigma^2}{\sqrt{m_{tt}m_{ss}}}\frac{z-h}{h} = \frac{2\pi\sigma^2}{\sqrt{|\boldsymbol{\Lambda}|}}\frac{z-h}{h}, \qquad (18)$$

where $\boldsymbol{\Lambda}$ is the covariance matrix of $\nabla\eta$. The total area covered by all the local maxima with amplitude z>h is given by

$$A_m(h) = \int_h^\infty EX_{lm}(z)\Gamma(z,h)dz = \frac{2\pi\sigma^2}{\sqrt{|\boldsymbol{\Lambda}|}}\int_h^\infty EX_{lm}(z)\frac{z-h}{h}dz. \qquad (19)$$

Further, the area A_s of the excursion set $A_{\eta,h}$ is given by

$$A(\eta \geq h) = A_S \int_h^\infty p(\eta = w)dw. \qquad (20)$$

where the pdf $p(\eta)$ is Gaussian. For h>>1, $A_{\eta,h}$ is the union of disjoint elliptical areas covered by only isolated local maxima above h (see Figure 4). Thus $A(\eta \geq h) = A_m(h)$ and (19) and (20) lead to the following Volterra integral equation of first kind

$$\int_h^\infty p(\eta = w)dw = \frac{2\pi\sigma^2}{A_S\sqrt{|\boldsymbol{\Lambda}|}}\int_h^\infty EX_{lm}(z)\frac{z-h}{h}dz \qquad (21)$$

for the unknown $EX_{lm}(z)$. Its solution proceeds by differentiating both members of (21) twice with respect to h, and setting h=z. This yield

$$EX_{lm}(z) = A_S\,(2\pi)^{-3/2}\sigma^{-2}|\boldsymbol{\Lambda}|^{1/2}(z/\sigma)^2\; e^{-(h/\sigma)^2/2}. \qquad (22)$$

From (15), integration by parts yields

$$EX_{\max}(h) \cong A_S\,(2\pi)^{-3/2}\sigma^{-2}|\boldsymbol{\Lambda}|^{1/2}\,h/\sigma\; e^{-(h/\sigma)^2/2}, \qquad (23)$$

which is identical to $\overline{EC(A_{\eta,h})}$ of (11) if we set $\xi = h/\sigma$.

UPCROSSINGS & MAXIMA

Consider now one-dimensional (1D) random processes. In this case, the EC of excursion sets counts the number of upcrossings. Thus, (14) simply states that the expected number of large maxima equals that of large h-upcrossings, implying the well known one-to-one correspondence between h-upcrossings and maxima at large thresholds. For two dimensional (2D) random fields this correspondence does not hold since upcrossings are contour levels. However, the definition of a 2D upcrossing is somehow vague. Can we define an appropriate 2D h-upcrossing for random fields so that the correspondence with large maxima is also one-to-one?

The answer to this question follows from the seminal work of Adler (1976) on generalizing upcrossings to higher dimensions. Without losing generality, consider the Gaussian field $\eta(x,y)$ on a new cartesian coordinate system (t,s) so that the covariance matrix Λ of $\nabla\eta$ is diagonal, viz.

$$\Lambda = \begin{bmatrix} m_{tt} & 0 \\ 0 & m_{ss} \end{bmatrix}, \qquad (24)$$

where m_{tt} and m_{ss} ($m_{tt} > m_{ss}$) are the second order spectral moments and the determinant $|\Lambda| = m_{tt}m_{ss}$. Note that the t-axis is along the principal direction θ (with respect to the original x axis) where the second spectral moment along θ attains its maximum. The partial derivatives $\partial_t\eta$ and $\partial_s\eta$ are thus uncorrelated and stochastically independent. With this setting in mind, a 2D h-upcrossing occurs at a point $P \in S$ if

i. a 1D h-upcrossing occurs along t ($\eta = h, \partial_t\eta > 0$ at P);

ii. η attains a 1D local maximum along s, i.e. η is convex along s ($\partial_s\eta = 0$, $\partial_{ss}\eta < 0$ at P).

Note that the extra condition (ii) guaranties that η is increasing locally at P. Further, this definition does not depend on the particular choice of the coordinate axes, and for large thresholds each 2D upcrossing corresponds uniquely to a large local maximum of η. Indeed, following Rice logic (Adler 1981), the expected number $EX_+(h)$ of 2D h-upcrossings is given by the following generalized Rice formula

$$\begin{aligned} EX_+(h) = A_S \int_{w_1=0}^{\infty}\int_{w_2=-\infty}^{0} w_1|w_2|\,\cdot \\ \cdot\, p(\eta = h, \partial_t\eta = w_1, \partial_s\eta = 0, \partial_{ss}\eta = w_2)dw_1dw_2 \end{aligned} \qquad (25)$$

where $p(\bullet)$ is the joint probability density function (pdf) of $\eta, \partial_t\eta, \partial_s\eta, \partial_{ss}\eta$. For an exact solution of (14) we refer to Adler (1981). Instead, an asymptotic solution for h>>1 can be derived as follows. By Gaussianity, $\partial_t\eta$ and $\partial_s\eta$ are independent of each other and from $\partial_{ss}\eta$ and η. This implies that

$$\begin{aligned} EX_+(h) = A_S \int_{w_1=0}^{\infty} w_1 p(\partial_t\eta = w_1)dw_1\,\cdot \\ \underline{\cdot\, p(\partial_s\eta = 0)\int_{w_2=-\infty}^{0}|w_2|p(\eta = h, \partial_{ss}\eta = w_2)dw_2}. \end{aligned} \qquad (26)$$

The first integral on the left is equal to $\sqrt{m_{tt}/(2\pi\sigma^2)}$, and the underlined terms equal the expected number, per unit length along s, of 1D local maxima with amplitude h. This is given, for large h, by $\sqrt{m_{ss}/(2\pi\sigma^2)}\,\xi\exp(-\xi^2/2)$, with $\xi = h/\sigma$ the dimensionless threshold. Since the determinant $|\Lambda| = m_{tt}m_{ss}$ is invariant by any axes rotation, we conclude that in general $EX_+(h)$ of (17) equals $EC(A_{\eta,h})$ of (11). Thus, for h>>1,

$$EX_+(h) \approx EX_{\max}(h) \approx \overline{EC(A_{\eta,h})}. \tag{27}$$

This proves the existence of a one-to-one correspondence between 2D upcrossings and large maxima as in 1D processes. Adler's result (11) is thus relevant for applications because large upcrossings or maxima of random fields can be counted by simply estimating the Euler characteristic of excursion sets.

EC OF OCEANIC SEA STATES

In the following we extend (13) to deal with the expected *EC* of excursion sets of spatial snapshots of oceanic sea states measured by **WASS** (see Figure 1). To properly model oceanic nonlinearities (Fedele 2008), we follow Tayfun (1986) and define the nonlinear wave surface η_{nl} over *S* as

$$\eta_{nl} = \eta + \frac{\mu}{2}\left(\eta^2 - \hat{\eta}^2\right), \tag{28}$$

where $\mu = \lambda_3/3$ is the wave steepness, which relates to the skewness λ_3 of η_{nl}, and $\hat{\eta}$ is the Hilbert transform of a normalized Gaussian field η. For ξ>>1, the excursion regions where $\eta_{nl} \geq \xi$ include just isolated local maxima. So, the structure of the excursion set can be related to the surface field locally to a maximum of η_{nl} with amplitude greater or equal to ξ. Assume that this occurs at $t = t_0$ and $s = s_0$. Then, the surface locally around that maximum is described by the nonlinear Slepian model defined by conditional process (Tayfun & Fedele 2007, Fedele 2008, Fedele & Tayfun 2009)

$$\eta_{nc} = \left\{\eta_{nl}(t,s) \middle| \eta_{nl}(t_0,s_0) \geq \xi\right\}, \tag{29}$$

that unfortunately does not have a straightforward explicit solution. A simplification of (29) stems from particular structure of the nonlinear surface η_{nl} as follows. Note that, from (28) it is clear that the nonlinear quadratic component of η_{nl} is phase-coupled to the extremes of the Gaussian η. So, a large maximum of η_{nl} greater or equal to ξ occurs simultaneously when η itself is at a large maximum with an amplitude greater or equal to, say, ξ_1. Thus, the conditional process (29), for $\xi_1 >> 1$, is equivalent to the simpler process (Tayfun & Fedele 2007, Fedele 2008, Fedele & Tayfun 2009)

$$\eta_{nc} = \left\{\eta_{nl}(t,s) \middle| \eta(t_0,s_0) \geq \xi_1\right\} = \xi_1 \Psi + \frac{\mu}{2}\xi_1^2\left(\Psi^2 - \hat{\Psi}^2\right), \tag{30}$$

where Ψ is the normalized covariance of η. From (30), the nonlinear crest occurs at ($t = t_0$, $s = s_0$), where $\Psi = 1$ and $\hat{\Psi} = 0$, and its amplitude is given by

$$\xi = \xi_1 + \frac{\mu}{2}\xi_1^2. \tag{31}$$

Thus, the expected *EC* of the excursion set $\{\eta_{nl} \geq \xi\}$ equal that of the *EC* of the excursion set $\{\eta \geq \xi_1\}$ of the Gaussian η. By the variable transformation (35), from (11) it follows that

$$\overline{EC(A_{\eta_{nl},\xi})} = N\frac{-1+\sqrt{(-1+2\mu\xi}}{\mu}\exp\left[-\frac{\left(-1+\sqrt{(-1+2\mu\xi}\right)^2}{2\mu^2}\right], \tag{32}$$

Where $N = A_S N_w$ is the total number of 'waves' over the area A_S. In Figure 5 it shown a realization of the nonlinear field η_{nl} (μ=0.1) over an area $A_S = 100^2\sigma^2$ covered by roughly *N*=436 waves. The nonlinear surface is computed from (32) using a Gaussian-shape spectrum for the linear η with spectral bandwidths $\nu_x = 1.17, \nu_y = 0.59$. Fig. 6 plots the observed *EC* against the threshold *h*. Further, the expected nonlinear *EC* in (36) is compared against that Gaussian (11). The simulated data agree well with the nonlinear model (36) whereas the Gaussian EC underestimates data for larger thresholds as expected.
We point out that the largest crest height h_n expected over the simulated area can be directly estimated from the observed EC without any knowledge of the associated wave spectrum. Indeed, h_n depends upon the number of waves *N* which is in general estimated from spectra. An alternative way to indirectly estimate N is provided by the observed EC diagram of Figure 6 and (36) used as an inverse formula for *N*. Table 1 reports such estimates for different values of the observed EC. Good agreement with the simulated value N=436 is found for large EC amplitudes, whereas the worst estimate is for EC=1.

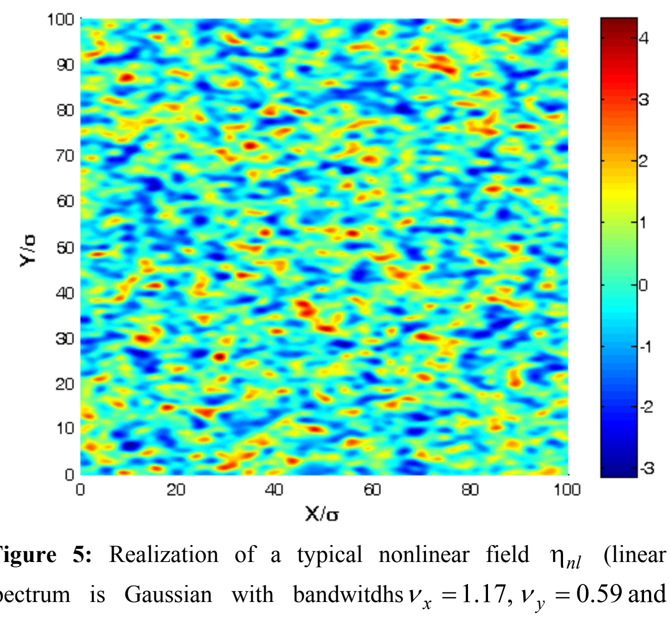

Figure 5: Realization of a typical nonlinear field η_{nl} (linear spectrum is Gaussian with bandwitdhs $\nu_x = 1.17, \nu_y = 0.59$ and steepness μ=0.1).

Hereafter, we analyze the EC of the oceanic video data collected by **WASS** of Figure 1. Figure 7 shows the observed EC against the threshold h and the expected theoretical ECs for the linear and nonlinear case. In Figure 8 is reported the same plot in log scale. The experimental data agree with the theoretical model (32).

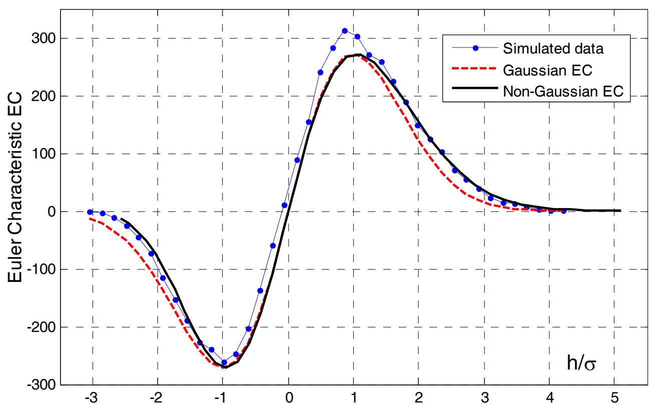

Figure 6: Observed EC from the simulated field of Fig. 5 and the expected EC against the threshold *h*.

Table 1: Estimates of N thorugh observed EC (exact N=436)

EC	ξ	ξ_1	Estimate N
200	1.75	1.62	~458
100	2.35	2.13	~450
1	4	3.41	~100

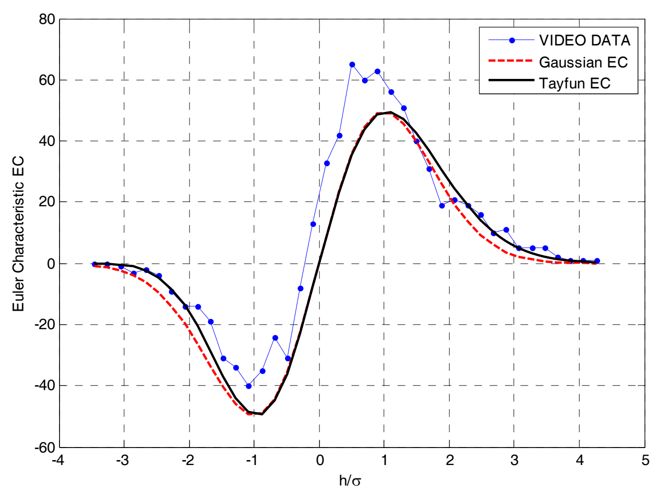

Figure 7. Observed EC and the expected EC against the threshold, as for the oceanic video data collected via **WASS** of Fig. 1.

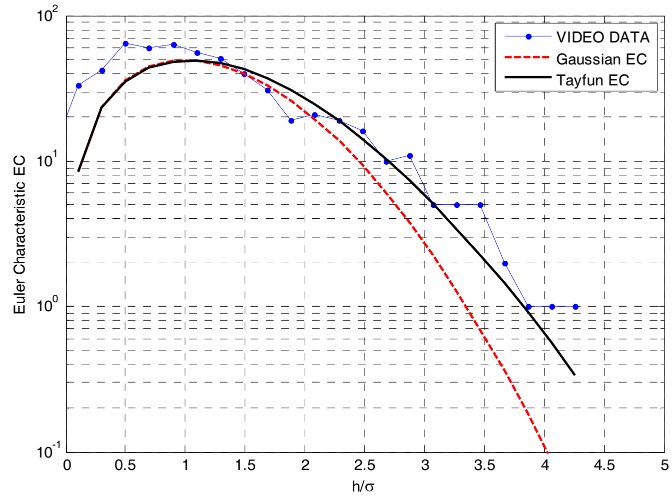

Figure 8: Same as in Figure 7.

CONCLUSIONS

We have presented an application of a novel variational image sensor **WASS** for the stereo reconstruction of wave surfaces. WASS technology, combined with statistical tools for the computation the Euler Characteristics of random excursion sets, provides reliable estimates of the largest crest of oceanic sea states.

ACKNOWLEDGMENTS

The authors would like to acknowledge Hailin Jin for providing source code that was partly used to obtain the results shown in this paper. Alvise Benetazzo is also grateful to Professor Ken Melville and Luc Lenain, of the Scripps Institution of Oceanography (SIO), San Diego, for the support received. We also thank Harald Krogstad for useful discussions and suggestions.

REFERENCES

Adler, R.J. 1976. On generalising the notion of upcrossings to random fields. *Advances in Applied Probability*, **27**(4):789-805.

Adler, R.J. 1981, *The Geometry of Random Fields*, New York: John Wiley.

Adler, R.J. 2000 On Excursion Sets, Tube Formulas and Maxima of Random Fields. *The Annals of Applied Probability* **10**(1), 1-74

Adler, R.J. & Taylor, J.E. 2007. *Random fields and geometry*. Springer Monographs in Mathematics Springer, New York.

Aldous, D. 1989. *Probability approximations via the Poisson Clumping Heuristic.* Springer-Verlag, New York.

Benetazzo, A. 2006. Measurements of short water waves using stereo matched image sequences Coastal Engineering, 53:1013-1032

Boccotti P. 2000. *Wave Mechanics for Ocean Engineering*. Elsevier Science, Oxford.

Faugeras O. & Keriven R. 1998 Variational principles, surface evolution, pde's, level set methods and the stereo problem. *IEEE Trans. on Image Processing*, **7**(3):336-344.

Fedele, F. 2008. Rogue Waves in Oceanic Turbulence. *Physica D* **237**, 14-17:2127-2131

Fedele F. & Tayfun, M.A. 2009. On nonlinear wave groups and crest statistics" *J. Fluid Mech.* **620,** 221-239

Forristall, G.Z. 2006, Maximum wave heights over an area and the air gap problem, *Proc. 25th International Conference on Offshore Mechanics and Arctic Engineering, OMAE2006-92022*, Hamburg.

Forristall, G.Z. 2007, Wave crest heights and deck damage in Hurricanes Ivan, Katrina and Rita, Offshore Technology Conference Proceedings, OTC 18620, Houston.

Gallego G, Benetazzo A., A. Yezzi, Fedele F. 2008 Wave spectra and statistics via a variational wave acquisition stereo system. OMAE2008-57160 paper, *Proc. ASME 27th Inter. Conf. Off. Mech. Arc. Eng.*, Estoril, Portugal.

Kac, M. & Slepian, D. 1959. Large excursions of Gaussian processes. *Ann. Math. Statist.* **30**,1215-1228.

Lindgren, G. 1970. Some properties of a normal process near a local maximum. Ann. Math. Statist. **4**(6),1870-1883.

Lindgren, G. 1972. Local maxima of Gaussian fields. Ark. fur Mat. **10**,195-218.

Ma, Y. Soatto, S., Kosecka, J., Shankar Sastry, S., 2004. *An invitation to 3-D vision: from images to geometric models.* Springer-Verlag New York

Piterbarg V. 1995 *Asymptotic Methods in the Theory of Gaussian Processes.* American Mathematical Society, ser. Translations of Mathematical Monographs, Vol. **148**, 205pp.

Socquet-Juglard, H., Dysthe, K., Trulsen, K., Krogstad, H.E. & Liu, J. 2005. Probability distributions of surface gravity waves during spectral changes. *J. Fluid Mech.* **542**, 195-216.

Tayfun, MA 1986. On narrow-band representation of ocean waves. Part I: Theory. J. Geophys. Res., (1(C6):7743-7752

Tayfun, M.A., & Fedele F. 2007. Expected shape of extreme waves in sea storms. *Proc. ASME 26th Inter. Conf. Off. Mech. Arc. Eng.*, San Diego, USA.

Worsley, K.J. 1995. Boundary corrections for the expected Euler characteristic of excursion sets of random fields, with an application to astrophysics. *Adv. App. Prob.*, **27**:943-959.

Zakharov VE. 1999. Statistical theory of gravity and capillary waves on the surface of a finite-depth fluid. European *Journal of Mechanics B-fluids* **18**(3):327-34

